

Time-Reversible Always Stable Predictor–Corrector Method for Molecular Dynamics of Polarizable Molecules

JÍŘÍ KOLAFA

*Institute of Physical Chemistry, Prague Institute of Chemical Technology,
166 28 Praha 6, Czech Republic*

Received 4 July 2003; Accepted 3 September 2003

Abstract: An improved method for classic molecular dynamics of polarizable molecules is proposed. The method uses a predictor, one evaluation of the electrostatic field per integration step, and relaxation (damping). The self-consistent solution is approximated with error of the second order (with respect to the timestep). The time reversibility (long-time energy conservation) error is of the $(2n - 1)$ th order, where n is the predictor length. The method is easy to implement, efficient, accurate, and suitable for any model of polarizability.

© 2003 Wiley Periodicals, Inc. J Comput Chem 25: 335–342, 2004

Key words: always stable predictor–corrector; induced dipole; polarizability; molecular dynamics; time reversibility

Introduction

An electrostatic field applied to a molecule distorts the electron cloud and thus induces dipoles (in general multipoles). This charge redistribution is fast so it is reasonable to assume, for the sake of molecular modeling, that it occurs instantaneously. In classic molecular dynamics (MD) we need to calculate electrostatic forces on all particles. Because the induced dipoles again create an electrostatic field, the problem of calculating the self-consistent field (SCF) in which all induced dipoles are in equilibrium with the field requires solving an implicit equation. Such a force field is no longer pairwise additive. The polarizability is essential for accurate description of properties as the solvation of ions or dielectric constant.

In the pioneering works^{1–3} the SCF was obtained by iterations. To avoid expensive iterations, it was proposed to predict the field on the basis of its knowledge from previous integration steps.^{4,5} This method with the Gear predictor improves efficiency, but the iteration procedure is not completely avoided. We call this method the *predicted iteration* method; it can be further optimized by damping.^{6,7}

The iterations in the predicted iteration method can be completely avoided by using a predictor of a special type accompanied by damping in the *always stable predictor–corrector* (ASPC) method.⁶ This early version of the method suffers by time irreversibility of the order of $\mathcal{O}(h^5)$, where h denotes the timestep.

In the extended Lagrangian method^{8,9} (inspired by the Car–Parrinello method^{10,11} for quantum mechanical systems and thus rather misleadingly known also by this name), new dynamic variables mimicking dipoles (one can imagine point charges attached

on springs) are added to the system. They follow changes in the electrostatic field and thus approximate the SCF.

All three above-mentioned methods are compared in detail in ref. 7. It is shown that the predicted iteration method is the most accurate but least efficient. The extended Lagrangian and ASPC methods are of the same speed. The extended Lagrangian method (with time-reversible integrator) exhibits better time reversibility while the ASPC method yields more accurate values of most thermodynamic quantities, although the systematic errors in energy, pressure, and radial distribution functions are small in both methods. However, the extended Lagrangian method fails for quantities directly related to induced dipoles and gives errors on the order of 10%.

Large fluctuations of the induced dipoles in the extended Lagrangian method can be suppressed by maintaining the weakly coupled subsystem of dynamic dipoles at lower temperature.⁹ This idea has been recently implemented by two Nosé–Hoover thermostats and optimized by multiple-timestep scheme to integrate efficiently the fast motion of dynamic dipoles.¹²

The induced dipoles or multipoles can be approximated in molecular modeling and simulations by finite-size multipoles (sets of point charges).⁸ A shell model or Drude oscillator model^{8,12} is based on point charges that change geometry, e.g., a dipole is approximated by a pair of opposite charges connected by a “spring.” Alternatively, a set of points of fixed geometry can adopt varying charges, which is called “fluctuating charge model.”^{8,13} Because the ASPC method is purely numerical, it can be applied to any polarization model.

Correspondence to: J. Kolafa; e-mail: kolafa@cesnet.cz

In this article we extend the ASPC method so that its time reversibility is improved. A series of predictors along with the corrector is derived with errors of the order of $\mathcal{O}(h^{2k+3})$, $k \geq 0$, where $k + 2$ is the total number of values from history (previous integration steps) needed to calculate the predictor. For $k = 1$ the original method⁶ is rederived.

Theory

Let us consider a set of N molecules (atoms, interaction sites) with partial charges, permanent dipoles, etc. An electric field \vec{E}_i acting on a molecule labeled i induces a dipole moment $\vec{\mu}_i$,

$$\vec{\mu}_i = \alpha \cdot \vec{E}_i \quad (1)$$

where α is the polarizability (scalar or tensor). Because the induced dipoles $\vec{\mu}_i$ on molecules i ($i = 1, \dots, N$) are also sources of an electrostatic field, we arrive at a set of N vector implicit equations for the SCF:

$$\vec{\mu}_i = \alpha \cdot \left(\sum_{j=1, j \neq i}^N \overset{\leftrightarrow}{T}_{ij} \cdot \vec{\mu}_j + \vec{E}_{\text{other}}(\vec{r}_1, \dots, \vec{r}_N) \right) \quad (2)$$

where

$$\overset{\leftrightarrow}{T}_{ij} = \frac{1}{r_{ij}^3} \left(\frac{3\vec{r}_{ij}\vec{r}_{ij}}{r_{ij}^2} - \overset{\leftrightarrow}{I} \right) \quad (3)$$

is the symmetrical dipolar tensor, $\overset{\leftrightarrow}{I}$ stands for unit tensor, \vec{r}_{ij} is the vector from point i to point j , and \vec{E}_{other} is the field caused by other charges in the system. This equation, or its equivalent for an alternate polarizability model, can be written concisely in the form

$$\mu = M(\mu; \vec{r}_1, \dots, \vec{r}_N) \quad (4)$$

where $\mu = (\vec{\mu}_1, \dots, \vec{\mu}_N)$ denotes the whole set of induced dipoles. This equation, interpreted as an assignment, represents a recipe to calculate the induced dipoles by direct iterations. The dependence on the configuration $\vec{r}_1, \dots, \vec{r}_N$ will be omitted in further text.

One step of the ASPC method^{6,7} consists of a predictor and a corrector. The *predictor* is a linear extrapolation [of local error $\mathcal{O}(h^2)$] with k additional terms (of the same local order),

$$\begin{aligned} \mu^p(t+h) = & 2\mu(t) - \mu(t-h) + \sum_{j=1}^k A_j \{ \mu(t-[j+1]h) \\ & - 2\mu(t-jh) + \mu(t-[j-1]h) \} \end{aligned} \quad (5)$$

where A_j , $j = 1, \dots, k$, are constants that are to be determined. While the order is apparent from this equation, for the sake of this article it is more convenient to use the equivalent form

$$\mu^p(t+h) = \sum_{j=0}^{k+1} B_{j+1} \mu(t-jh) \quad (6)$$

where

$$B_j = A_j - 2A_{j-1} + A_{j-2} \quad (7)$$

and, to simplify notation, we define $A_0 = -1$, $A_{-1} = 0$.

The *corrector* contains one evaluation of the right side, damped by using relaxation with parameter ω ,

$$\mu(t+h) = \omega M(\mu^p(t+h)) + (1-\omega)\mu^p(t+h) \quad (8)$$

Time Reversibility

A time-reversible MD method does not exhibit any long-time energy drift that is advantageous in practical simulations. The popular Verlet method^{14,15} and its variants (leap-frog, velocity Verlet) are symplectic and therefore time reversible for a certain class of potentials; although they are no longer exactly time reversible for potentials with singularities (like division by zero at zero atom–atom distance), their reversibility is still more than sufficient in practice. It is advantageous to combine the ASPC method for induced dipoles with the Verlet integration of the equations of motion because both are second-order methods.

To study the error of the method and consequently the time reversibility, let us Taylor expand both $\mu^p(t+h)$ on the left side of (6) and all $\mu(t-jh)$ on the right side and subtract both sides. The error of the predictor is

$$\sum_{l=0}^{\infty} \frac{(-h)^l}{l!} C_l \mu^{(l)}(t) \quad (9)$$

where

$$C_l = \sum_{j=0}^{k+1} B_{j+1} j^l \quad (10)$$

The terms at even powers of h in (9) are time reversible (because replacing $-h$ by h does not change the sign) while the odd terms cause time irreversibility. Our aim is therefore to find, for given length of the predictor k , numbers A_j , $j = 1, \dots, k$, so that as many odd terms C_l as possible are zero. Because we have k parameters to determine, and $C_1 = 0$ already for $k = 0$, it is possible to nullify terms $C_3, C_5, \dots, C_{2k+1}$.

It is shown in the Appendix that the solution of these equations is

Table 1. Coefficients of the ASPC Method and the (Unoptimized) Relaxation Parameter ω .

k	Time reversal	B_1	B_2	B_3	B_4	B_5	B_6	ω
0	$\mathcal{O}(h^3)$	2	−1					2/3
1	$\mathcal{O}(h^5)$	2.5	−2	0.5				0.6
2	$\mathcal{O}(h^7)$	2.8	−2.8	1.2	−0.2			4/7
3	$\mathcal{O}(h^9)$	3	−24/7	27/14	−4/7	1/14		5/9
4	$\mathcal{O}(h^{11})$	22/7	−55/14	55/21	−22/21	5/21	−1/42	6/11

$$\begin{aligned}
A_1 &= \frac{2k}{k+3} \\
A_2 &= -\frac{3k(k-1)}{(k+3)(k+4)} \\
A_3 &= \frac{4k(k-1)(k-2)}{(k+3)(k+4)(k+5)} \\
A_4 &= -\frac{5k(k-1)(k-2)(k-3)}{(k+3)(k+4)(k+5)(k+6)} \\
&\dots \\
A_i &= 0 \quad \text{for } i > k
\end{aligned} \tag{11}$$

or, equivalently,

$$\begin{aligned}
B_1 &= 1(4k+6) \frac{1}{(k+3)} \\
B_2 &= -2(4k+6) \frac{(k+1)}{(k+3)(k+4)} \\
B_3 &= 3(4k+6) \frac{(k+1)(k+0)}{(k+3)(k+4)(k+5)} \\
B_4 &= -4(4k+6) \frac{(k+1)(k+0)(k-1)}{(k+3)(k+4)(k+5)(k+6)} \\
&\dots \\
B_i &= 0 \quad \text{for } i > k+2
\end{aligned} \tag{12}$$

Stability

Stability means that errors (caused by higher-order terms than those taken into account by the predictor along with rounding, cutoff, and other errors) do not cumulate during the predictor–corrector procedure but decrease as fast as possible. It remains to be shown that (with appropriate choice of ω) the proposed method is stable.

Stability of integrators for ordinary differential equations of order n is studied by means of homogeneous equation $y^{(n)} = \lambda y$.^{16,17} Analogously, we will use the ASPC method to solve equation $M(\mu) = 0$ for the following “primitive” right side:

$$M(\mu) = \lambda \mu \tag{13}$$

where now μ is a scalar and λ , $|\lambda| < 1$, stands for the highest eigenvalue of linearized operator M ; it follows from the symmetry of tensor (3) that this operator is symmetrical and thus all its eigenvalues are real. While λ can be eliminated from differential equations by a time transformation, the same trick cannot be applied to the “zero-order differential equation” (13) and the whole

range of possible $\lambda \in (-1, 1)$ must be in general taken into account.

The solution (fixed point) of (13) is $\mu = 0$ and therefore the value of $\mu(t)$ equals the error. The predictor (5) and the corrector (8) with M given by (13) represent a recipe for how to calculate the error $\mu(t+h)$ using $\mu(t)$, $\mu(t-h)$, etc. In other words, the error propagation is described by a linear recurrence. The characteristic equation of this recurrence is

$$\xi^{k+2} = \lambda_\omega \sum_{l=1}^{k+2} B_l \xi^{k+2-l} \tag{14}$$

where

$$\lambda_\omega = \lambda \omega + (1 - \omega) \tag{15}$$

The convergence or divergence of the predictor is linear with the quotient given by the maximum (in absolute value) root ξ_{\max} of eq. (14). The condition of stability is thus $|\xi_{\max}| < 1$.

If we do not know the convergence rate of the SCF equation, we can only assume that $\lambda \in (-1, 1)$ because a physically correct system cannot diverge (a divergence is sometimes called a “polarization catastrophe”). The interval $\lambda \in (-1, 1)$ maps to $\lambda_\omega \in (1 - 2\omega, 1)$. It will be shown in the Appendix that for

$$\omega = \frac{k+2}{2k+3} \tag{16}$$

all roots of the characteristic equation for all $\lambda \in (-1, 1)$ lie in a unit circle in the complex plane. The predictor coefficients (12) along with the relaxation parameter (16) complete the proposed method.

The ASPC methods for several lowest values of k are summarized in Table 1. The $k = 0$ method has a bad energy conservation; the $k = 1$ method is identical to the method derived in ref. 6.

The values of ω given by (16) ensure stability for any converging equation for the SCF. In particular systems the convergence may be better, the range of eigenvalues is confined to a certain interval, $\lambda \in (\lambda_{\min}, \lambda_{\max}) \subset (-1, 1)$, and consequently larger values of ω do not cause instability. Because larger values of ω improve accuracy, it is desirable to use the largest ω guaranteeing stability. To estimate the optimum ω , it is possible to study convergence properties of the SCF iterations and estimate the minimum and maximum eigenvalues.⁶ From these values, one can

derive ω ensuring convergence. Another approach, applied in this work, is to determine the optimum ω by trial and error.

Test

To test the method, we simulated the RPOL (Revised Polarizable) model of water¹⁸ at ambient conditions (temperature 25°C, density 0.997 g cm⁻³). This three-site model with all sites polarizable consists of oxygen and two hydrogens in rigid geometry. The OH distance is 1 Å, HOH angle 109.5°, partial charges (polarizabilities) of O and H are $-0.73e$ (0.528 Å³) and $+0.365e$ (0.178 Å³), respectively, and the O–O Lennard–Jones interaction has the collision diameter $\sigma = 3.196$ Å and minimum energy (in absolute value) $\varepsilon = 0.16$ kcal/mol.

A standard cubic periodic sample of 256 molecules and constant volume was used. The electrostatic interactions were calculated by the Ewald summation with the r -space cutoff of one half of the box size (9.87 Å), the separation parameter $\alpha = 0.358/\text{Å}$, and the k -space cutoff $K = 7.1$. The induced dipoles were approximated by finite-size dipoles (shell or Drude model) with the shell charge of $-1000e$.^{6,8,12} The equations of motions were integrated by the Verlet method with timestep of $h = 0.001$ ps. The configurations were well equilibrated before running the tests. The simulations were performed using MACSIMUS.¹⁹

Four quantities were monitored. The standard thermodynamic quantities are represented by the residual internal energy E and virial pressure P . The induced dipoles are studied by the mean squared value of the induced dipole, $\langle \mu_{\text{ind}}^2 \rangle$. The simulation error in the induced dipoles is expressed by

$$\delta\mu = \langle (\mu_{\text{ind}} - \mu_{\text{SCF}})^2 \rangle^{1/2} \quad (17)$$

where μ_{SCF} is obtained by iterations with the error threshold of 10^{-6} Debye. All quantities were sampled by 10 MD steps, i.e., by 0.01 ps.

Optimizing the ASPC Method

We used a trial-and-error approach to optimize the relaxation parameter ω and ran several short simulations (of 5 ps) with increasing ω until divergence was detected. The results are collected in Figure 1. It is seen that error $\delta\mu$ decreases with increasing ω until the limit of stability is reached. Because this limit depends on the configurations and fluctuates in time, we set the optimum ω to the values by 0.03 less than the obtained stability limit values.

We used error $\delta\mu$ to detect the stability limit. This quantity is somehow difficult to calculate because iterations of the SCF are needed. Nevertheless, equivalent results can be obtained by monitoring the energy conservation error or one-step error in induced dipoles, which are easy to calculate. In addition, shorter runs than the used 5 ps are sufficient to determine the optimum ω provided that the starting configurations are well equilibrated.

Energy Conservation

Several short (10 ps) tests in the MD microcanonical ensemble were performed for a series of methods to study the energy

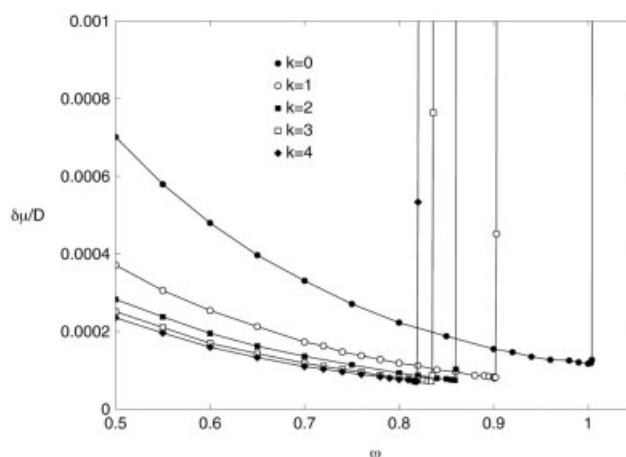


Figure 1. Error in induced dipoles $\delta\mu$ as a function of the relaxation parameter ω , calculated by the ASPC methods.

conservation. All runs started from the same initial configuration. The plots of total energy versus time (to 1 ps) are shown in Figure 2. It is seen that the energy drift, which is considerable for the $k = 0$ method, decreases and becomes undetectable for $k = 3$.

Similar runs for doubled timestep ($h = 0.002$ ps) exhibit much larger drifts. The data are collected in Table 2 along with the estimated orders of long-time energy conservation. To do this, the data were fitted to polynomials (for larger k where the decrease of energy cannot be accurately described by a linear function) or to a linear function; the drift is a tangent at $t = 0$.

Because the data in Table 2 were obtained by single runs, they do not represent ensemble averages with error estimates based on ensemble sampling. Therefore, the observed differences of the “experimental” orders from the theoretical ones are acceptable and we may conclude that the ASPC methods exhibit theoretically predicted long-time energy conservation.

Thermodynamics

To reveal possible systematic errors in thermodynamic quantities caused by the ASPC method we ran several 2-ns simulations. To avoid a change of the thermodynamic state because of energy drift, we used the Berendsen (friction) thermostat.^{14,15} This thermostat is more suitable for our purposes than the Nosé–Hoover thermostat,²⁰ which violates time reversibility of the (velocity) Verlet method unless special tricks are used.¹⁴ Heat-bath methods based on drawing new velocities at random from the Maxwell–Boltzmann distribution, as the Andersen method,²¹ violate the predictor chain and cannot be used either.

The Berendsen thermostat is not without drawbacks either. Short characteristic time (large coupling) causes bad equipartition between translational and rotational degrees of freedom.²² Therefore, we used a relatively long thermostat characteristic time of 1 ps.

In Table 3 results obtained by the ASPC methods, $1 \leq k \leq 4$, both with optimized and unoptimized ω , are compared with the predicted iteration method considered as the benchmark (accuracy limit of two consecutive iterations of the induced dipoles was set to $\varepsilon = 10^{-5}$ Debye). All other simulation conditions were identi-

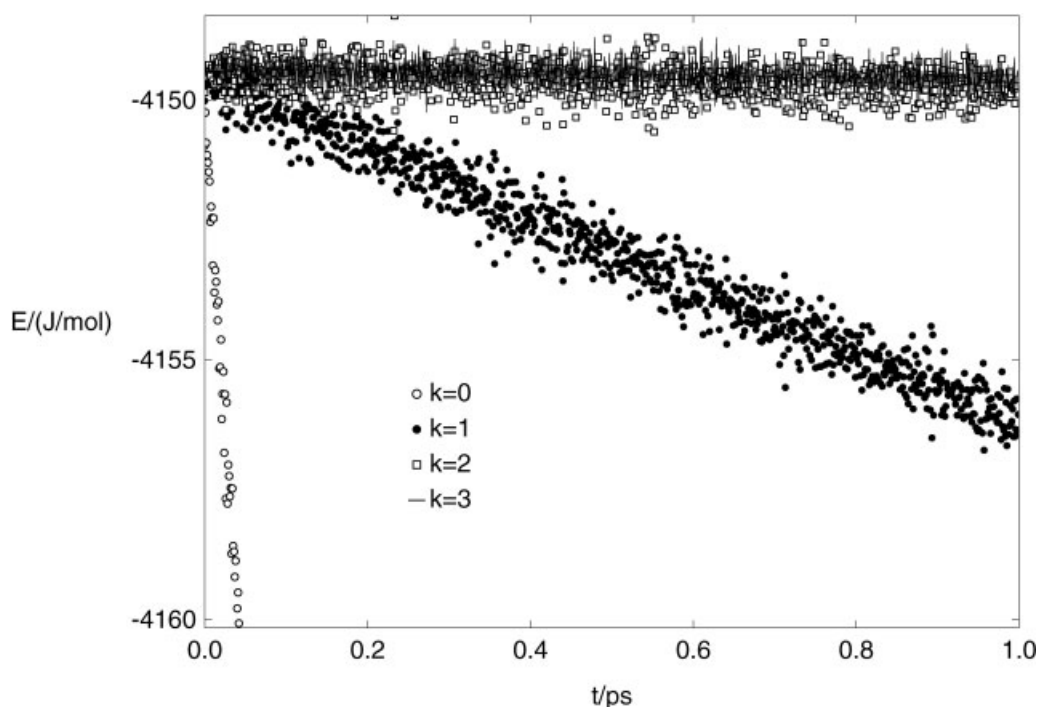


Figure 2. Total energy as a function of time for the ASPC methods with $h = 0.001$ ps.

cal: the same Ewald parameters, the same time constant of the thermostat (1 ps), and the same temperature parameter of the thermostat $T = 298.15$ K.

It is seen that the averaged kinetic temperature differs by about 0.15 K from the thermostat constant $T = 298.15$ K. This is a finite size effect caused by fluctuations of the kinetic temperature around the thermostat value. The magnitude of this deviation is of the order of $1/f$, where $f = 6N$ is the number of degrees of freedom. It is not possible to correct for this effect because the Berendsen thermostat does not generate a canonical (nor any other well-defined) ensemble. We thus rather compare the average kinetic

temperature of the predicted iteration method with the ASPC method results. Only the temperature of the $k = 1$ method exhibits a systematic deviation as a consequence of poor energy conservation; this difference would be smaller for larger thermostat coupling. The $k > 1$ methods do not exhibit any measurable temperature difference.

As regards energy, pressure, and averaged induced dipoles, the deviations from the benchmark values are small; the relative deviations are about 0.1% (but pressure because its relative error is not a well-defined quantity). The deviations in energy and pressure are detectable (at the 95% confidence level) for $k = 1$ only and are at the limit of detectability at this confidence level for the optimized version of $k = 2$. The averaged induced dipoles show just detectable deviations also for the unoptimized $k = 3$ and $k = 4$ ASPC methods. The ASPC errors in averaged induced dipoles are nevertheless by two orders of magnitude smaller than the extended Lagrangian method results⁷ unless the induced dipole subsystem is kept at low temperature.^{9,12}

The error of the induced dipoles $\delta\mu$ is a control quantity of the simulation. Its value for the predicted iteration method is in agreement with the iteration accuracy. For the unoptimized ASPC methods it is about two or three times larger than for optimized ω . This error is as large as 20% for the extended Lagrangian method.⁷

Computational Overhead and Memory Requirements

The implementation of the ASPC method needs one evaluation of the electrostatic field per integration step and several operations per particle. The computational overhead is then of the order of $\mathcal{O}(N)$ as for the extended Lagrangian method.

Table 2. Energy Drift dE/dt at $t = 0$ (Obtained by Fitting the 10-ps Development of Total Energy to Polynomial of Degree n) and the Calculated Order of Long-Time Energy Conservation.

k	$h = 0.002$			$h = 0.001$		
	n	(dE/dt) (J mol ⁻¹ ps ⁻¹)		n	(dE/dt) (J mol ⁻¹ ps ⁻¹)	Order
0	5 ^a	-1464		4	-203.5	2.85
1	4	-180.9		2	-5.32	5.09
2	2	-27.99		1	-0.207	7.07
3	1	-7.26		1	-0.018	8.6
4	1	-2.94		1	-0.005	9

The accuracy of the presented data, as calculated from the regression, is within ± 2 in the last digit.

^a3-ps run.

Table 3. Selected Thermodynamic Properties of the RPOL Model of Water Calculated by Different Methods.

Method	ω	t (ns)	T_{kin} (K)	E (kJ mol ⁻¹)	P (MPa)	$10^5 \delta\mu$ (D)	$\langle\mu_{\text{ind}}^2\rangle^{1/2}$ (D)
Predicted iteration	0.95	2.5	298.00(7)	-42.155(8)	-43.1(8)	0.04	0.64222(16)
ASPC, $k = 1$	0.87	2.1	297.57(8)	-42.218(9)	-44.3(10)	9.19	0.64321(20)
ASPC, $k = 2$	0.83	2.1	297.98(8)	-42.184(9)	-41.6(9)	8.29	0.64286(15)
ASPC, $k = 3$	0.80	2.1	298.02(8)	-42.157(8)	-41.6(10)	8.21	0.64242(16)
ASPC, $k = 4$	0.79	2.1	298.03(8)	-42.163(8)	-42.6(9)	7.92	0.64244(16)
ASPC, $k = 1$	0.60	2.2	297.36(8)	-42.202(8)	-44.8(9)	25.37	0.64303(15)
ASPC, $k = 2$	4/7	2.1	298.01(8)	-42.160(8)	-42.8(9)	21.82	0.64239(17)
ASPC, $k = 3$	5/9	2.1	298.01(8)	-42.168(8)	-41.5(11)	20.43	0.64266(16)
ASPC, $k = 4$	6/11	2.1	298.01(8)	-42.181(9)	-42.1(9)	19.69	0.64281(16)

ω is the relaxation parameter (8), t total length of the simulation, T_{kin} averaged kinetic temperature, E residual internal energy, P pressure, $\delta\mu$ error of simulation induced dipoles (17), and μ_{ind} denotes the induced dipole. Values in parentheses are estimated statistical uncertainties (standard deviations) in the units of the last significant digit.

The memory requirements depend on the dipole model and other implementation details. The recommended $k = 2$ ASPC method needs $4N$ vectors to store the history, compared to $2N$ (dipole and time derivative) for the standard extended Lagrangian method. Because $2N$ is needed to store the particles and velocities themselves, and usually (according to the implementation, constraint dynamics, etc.) a few other N are required, the memory requirements of the ASPC method are by 50–25% larger than that of the standard extended Lagrangian method.

Conclusions

We derived a series of methods for classic MD of polarizable molecules and showed that the results are subject to small systematic errors of the second order. The methods require one evaluation of the right side per integration step and are thus of the same efficiency as the extended Lagrangian (Car–Parrinello-like) method but approximate the induced dipoles much better. Unlike the Car–Parrinello-like methods with double thermostat,¹² the ASPC method works efficiently without multiple timestep integration schemes.

The ASPC methods can be used for any polarizability model or approximation (scalar or tensor, multipole, shell or Drude model, fluctuation charge model). In general, they can be used for numerical solution of sets of ordinary differential equations (of any order) with the right side containing an implicit equation of the SCF type provided that the linearized SCF operator is symmetrical. The ASPC methods are suitable for dynamics systems if time reversibility is more important than the order of the method.

The ASPC methods with $k > 1$ have sufficient time reversibility. A recommended method for integration of the equations of motion to accompany the proposed ASPC method for induced dipoles is the Verlet method because it is also of the second order and has good time reversibility.

We recommend the method with $k = 2$ as a compromise between complexity and a good time reversibility. The predictor is

$$\mu^p(t+h) = 2.8\mu(t) - 2.8\mu(t-h) + 1.2\mu(t-2h) - 0.2\mu(t-3h) \quad (18)$$

The always stable corrector is given by (8) with $\omega = 4/7$, although larger values of ω may lead to smaller errors in particular simulations.

If good time reversibility is required, and other sources of irreversibility are avoided, the methods with $k > 2$ may be useful.

Acknowledgment

This work was supported by the The Ministry of Education, Youth and Sports of the Czech Republic under Project LN00A032 (Structure and Dynamics of Complex Molecular Systems and Biomolecules).

Appendix

Time Reversibility

We first prove that $C_l = 0$ [eq. (10)] for all odd $l \leq 2k + 1$ with B_l given by eq. (12). After substituting $n = k + 1$ to simplify the products, expression (12) becomes

$$B_j = (-1)^{j+1}j(4n+2) \frac{n(n-1) \cdots (n+2-j)}{(n+2)(n+3)(n+4) \cdots (n+1+j)} \\ = (-1)^{j+1}j \binom{2n+2}{n+1-j} / \binom{2n}{n} \quad (19)$$

for $0 < j < n + 2$ and $B_j = 0$ otherwise. Equation $C_l = 0$ is then equivalent to

$$\binom{2n+2}{n} 1^{l+1} - \binom{2n+2}{n-1} 2^{l+1} + \cdots \pm \binom{2n+2}{0} (1+n)^{l+1} = 0 \quad (20)$$

For even $l + 1$, i.e., odd l , one can write this equation twice: In one instance replace 1^{l+1} by $(-1)^{l+1}$, 2^{l+1} by $(-2)^{l+1}$, etc., and add term $0 = \binom{2n+2}{n+1} 0^{l+1}$. The resulting equation reads as

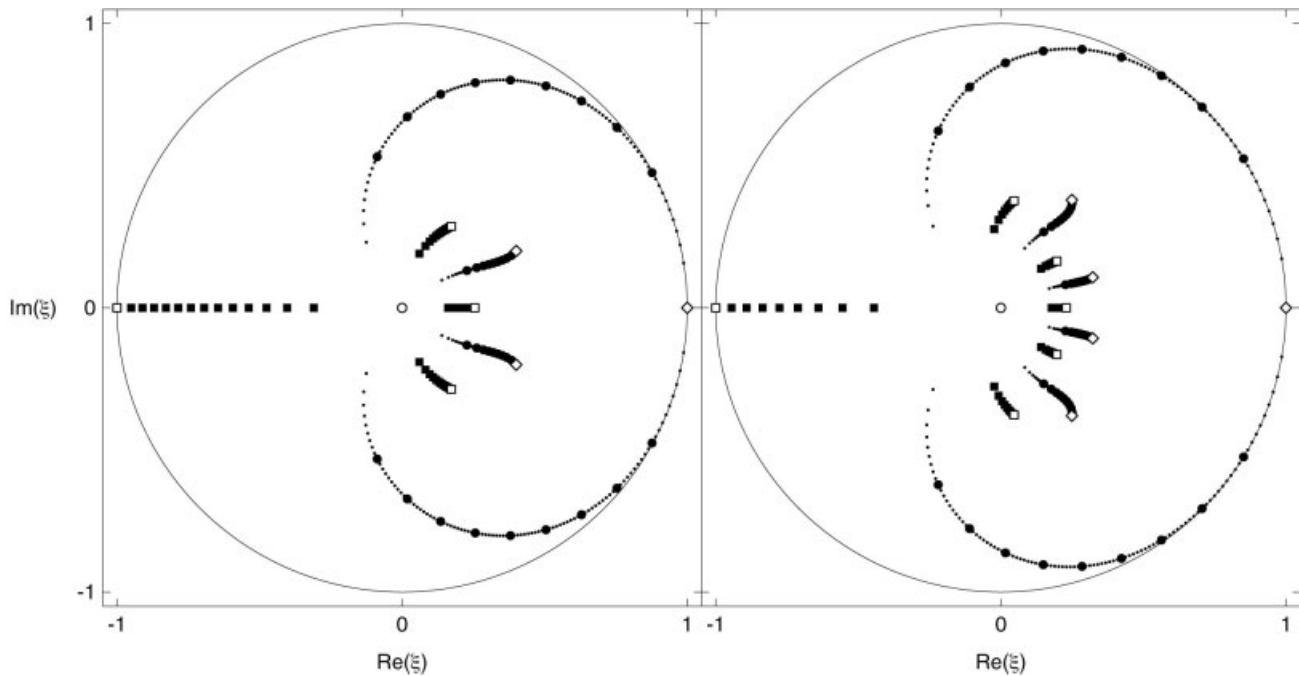


Figure 3. Roots of the characteristic eq. (14) for $k = 2$ (left) and $k = 4$ (right) and a series of $\lambda_\omega \in [-1/(2k+3), 1]$, which corresponds to $\lambda \in [-1, 1]$ for ω given by (16). Open square, $\lambda_\omega = -1/(2k+3)$; solid squares, $\lambda_\omega \in (-1/(2k+3), 0)$, by 0.01; open circle, $\lambda_\omega = 0$; dots, $\lambda_\omega \in (0, 1)$, by 0.01 (every 10th enlarged); diamond, $\lambda_\omega = 1$.

$$\sum_{i=0}^{2n+2} \binom{2n+2}{i} (-1)^i (i-n-1)^{l+1} = 0 \quad (21)$$

This is the operator of $(2n+2)$ th difference applied to function $f(j) = (j-n-1)^{l+1}$ and therefore the result is zero for $2n+2 > l+1$, i.e., $l \leq 2k+1$.¹⁷ [The difference operator is defined by $\Delta f(j) = f(j) - f(j-1)$. A degree of a polynomial is decreased by one by applying this operator. The sum in (21) then equals $\Delta^{2n+2} f(j)$ because powers of the difference operator contain binomial coefficients with alternating signs that can be shown by using the Pascal triangle.]

Roots of the Characteristic Equation

We first investigate the two limiting cases, $\lambda = -1$ [and therefore $\lambda_\omega = -1/(2k+3)$] and $\lambda = +1$ (and therefore $\lambda_\omega = 1$).

To show that $\xi = -1$ is the root of eq. (14) for $\lambda_\omega = -1/(2k+3) = -1/(2n+1)$, we have to show that

$$(-1)^{n+1} = -\frac{1}{2n+1} \sum_{j=1}^{n+1} B_j (-1)^{n+1-j} \quad (22)$$

By inserting B_j given by (19) we obtain the equivalent form

$$(2n+1) \binom{2n}{n} = \sum_{j=1}^{n+1} j \binom{2n+2}{n+1-j} \quad (23)$$

This formula can be proven by induction. It is easy to show that (23) holds true for $n = 0$. As the induction step, we replace the binomial coefficients on the right side of (23) by

$$\binom{2n+2}{n+1-i} = \binom{2n}{n-1-i} + 2 \binom{2n}{n-i} + \binom{2n}{n+1-i} \quad (24)$$

A rearrangement of indices leads to four times the right side for n instead of $n+1$ plus an extra term $\binom{2n}{n}$,

$$\begin{aligned} \sum_{j=1}^{n+1} j \binom{2n+2}{n+1-j} &= 4 \sum_{i=1}^n j \binom{2n}{n-j} + \binom{2n}{n} \\ &= 4(2n-1) \binom{2n-2}{n-1} + \binom{2n}{n} \\ &= (2n+1) \binom{2n}{n} \end{aligned} \quad (25)$$

To show that $\xi = 1$ is a root of eq. (14) for $\lambda_\omega = 1$, we insert again B_j into (14). The expression to be proven reads as

$$\binom{2n}{n} = \sum_j^{n+1} j(-1)^{j+1} \binom{2n+2}{n+1-j} \quad (26)$$

Inserting (24) into the right side and rearranging causes all terms but $\binom{2n}{n}$ to cancel out.

It remains to be shown that all other roots of the characteristic equation for all $\lambda \in (-1, 1)$ are in the absolute value less than unity, i.e., the above-found two roots are the limiting cases of the worst convergence. We do not know a mathematical proof of this statement, but we verified it numerically; a copy of the program is available upon request. For all $k < 15$ and a series of λ_ω from interval $(-1/(2k + 3), 1)$ we have found that all roots of the characteristic equation lie in the unit circle. Examples of the roots for $k = 2$ and $k = 4$ are shown in Figure 3.

References

1. Vesely, F. J. *J Comput Phys* 1977, 24, 361.
2. Pollock, E. L.; Alder, B. J.; Patey, G. N. *Physica* 1981, 108A, 14–26.
3. Van Belle, D.; Couplet, I.; Prevost, M.; Wodak, S. J. *J Mol Biol* 1987, 198, 721–735.
4. Ahlström, P.; Wallqvist, A.; Engström, S.; Jönsson, B. *Mol Phys* 1989, 68, 563–581.
5. Ruocco, G.; Sampoli, M. *Mol Phys* 1994, 82, 875–886.
6. Kolafa, J. *Mol Simul* 1996, 18, 193–212.
7. Genzer, J.; Kolafa, J. *J Mol Liq* (in press).
8. Sprik, M.; Klein, M. L. *J Chem Phys* 1988, 89, 7556–7560.
9. Sprik, M. *J Chem Phys* 1991, 95, 6762–6769.
10. Car, R.; Parrinello, M. *Phys Rev Lett* 1985, 55, 2471–2474.
11. Remler, D. K.; Madden, P. A. *Mol Phys* 1990, 70, 921–966.
12. Lamoureux, G.; Roux, B. *J Chem Phys* 2003, 119, 3025–3039.
13. Rick, S. W.; Stuart, S. J.; Berne, B. J. *J Chem Phys* 1994, 101, 6141–6156.
14. Frenkel, D.; Smit, B. *Understanding Molecular Simulation*; Academic: New York, 2002.
15. Allen, M. P.; Tildesley, D. J. *Computer Simulation of Liquids*; Clarendon Press: Oxford, UK, 2002.
16. Gear, C. W. *Numerical Initial Values Problems in Ordinary Differential Equations*; Prentice-Hall: Englewood Cliffs, NJ, 1971.
17. Ralston, A. *A First Course in Numerical Analysis*; McGraw-Hill: New York, 1965.
18. Dang, L. X. *J Chem Phys* 1992, 97, 2659–2660.
19. MACSIMUS; <http://www.icpf.cas.cz/jiri/macsimus>.
20. Hoover, W. G. *Phys Rev* 1985, 31A, 1695–1697.
21. Andersen, H. C. *J Chem Phys* 1980, 72, 2384–2393.
22. Harvey, S. C.; Tan, R. K. Z.; Cheatham, E. T. III. *J Comput Chem* 1998, 19, 726–740.